The influence of incommensurate modulation on the optical properties of $((CH_3)_4N)_2CuCl_4$

1995 J. Phys.: Condens. Matter 7 8119

(http://iopscience.iop.org/0953-8984/7/42/009)

J. Phys.: Condens. Matter 7 (1995) 8119–8138. Printed in the UK

The influence of incommensurate modulation on the optical properties of $((CH_3)_4N)_2CuCl_4$

M Kremers and H Meekes

RIM Laboratory of Solid State Chemistry, University of Nijmegen, Toernooiveld, 6525 ED Nijmegen, The Netherlands

Received 26 June 1995, in final form 4 August 1995

Abstract. This paper reports on the measurement of the optical properties of incommensurately modulated $((CH_3)_4N)_2CuCl_4$ by using the High Accuracy Universal Polarimeter. With this technique it is possible to measure, simultaneously, linear birefringence, linear dichroism, circular birefringence, circular dichroism and the rotation of the optical indicatrix. Two different samples are used. The orientation of the first sample allows for the measurement of the gyration tensor element g_{33}. In the other sample g_{13} can be measured. The optical effects are studied as a function of temperature, both in a region of zero linear dichroism and in a region of finite linear dichroism. The measurements reveal that the crystals have a low defect concentration. The presence of the incommensurate modulation is clearly revealed by the linear birefringence. The linear dichroism, on the other hand, appears to be unaffected by the modulation. It is interesting that if one averages the effect of the incommensurate modulation a crystal structure is obtained that is believed to be orthorhombic and centrosymmetric. Two effects are observed that are forbidden by the symmetry of this average structure. One of them is the rotation of the optical indicatrix, which contradicts an orthorhombic symmetry. The other is the onset of non-zero optical activity, approximately halfway through the incommensurate phase. In centrosymmetric media this effect is not allowed to occur. The observed temperature dependence of the optical activity g_{13} differs from the behaviour measured by other authors. It is discussed whether the observed effects can be attributed to a symmetry breaking by the incommensurate modulation.

1. Introduction

Tetramethylammonium tetrachloro-cuprate $((CH_3)_4N)_2CuCl_4$ [1, 2] is a member of the family of A_2BX_4-type crystals that show a phase transition from a β-K_2SO_4 structure into an incommensurately modulated phase. The modulation wave vector of $((CH_3)_4N)_2CuCl_4$, $q = (2 + \delta)c^*/3$ with $\delta \approx 0.02$, is approximately constant in the incommensurate phase [3]. Due to the incommensurateness of the modulation wave vector the three-dimensional lattice translational symmetry is broken in the incommensurate phase. This phase is often considered to be an intermediate phase between the β-K_2SO_4-type phase and a so-called lock-in phase. In the latter, the modulation becomes commensurate with the lattice. Therefore a superstructure is formed. The resulting structure has, again, three-dimensional lattice translational symmetry and is usually ferroelectric. In the case of $((CH_3)_4N)_2CuCl_4$, however, the lock-in phase is ferroelastic [4]. Another lock-in phase exists at lower temperatures [5].

Due to the broken lattice translational symmetry it is not possible to use a normal space group description for the incommensurate phase. The crystal can, however, be embedded in a so-called superspace, where the lattice translational symmetry is restored.

0953-8984/95/428119+20$19.50

The symmetry can, consequently, be described by means of a so-called superspace group [6–9]. It is, often, even possible to use the same superspace group for the embedding of the other (commensurate) phases [10]. To our knowledge, the superspace group symmetry of the incommensurate phase of $((CH_3)_4N)_2CuCl_4$ has not been determined experimentally. Nevertheless, it is believed that the only superspace group that allows for the, known, normal space group symmetries of the other phases is $Pcmn(00\gamma)(1s\bar{1})$ [11, 12]. The parameter γ characterizes the modulation wave vector as $q = \gamma c^*$. Note that this superspace group is equivalent to $Pcmn(00\gamma)(ss\bar{1})$ with the modulation wave vector $c^* - q$ instead of q. If, in the incommensurate phase, the effect of the modulation is averaged one has an orthorhombic and centrosymmetric structure. For the related compound $((CH_3)_4N)_2CuBr_4$ the superspace group is known to be $Pcmn(\alpha 00)(\bar{1}s1)$ [13]. The average structure of this crystal is also orthorhombic and centrosymmetric. It is the aim of this paper to investigate whether optical effects can be observed in the incommensurate phase of $((CH_3)_4N)_2CuCl_4$ that are not allowed by the symmetry of the average structure. These effects then have to be caused by the presence of the incommensurate modulation.

Recently, we have investigated the optical properties of another member of the A_2BX_4 family, $((CH_3)_4N)_2ZnCl_4$ [14], which also has the superspace group symmetry $Pcmn(00\gamma)(1s\bar{1})$. We searched for the presence of optical activity in the incommensurate phase, because this effect is a sensitive test for the symmetry. Due to the finiteness of the wavelength of the light in the optical region, (weak) spatial dispersion contributes to the propagation of light in crystals. It is understood that this causes optical activity. It is a third-rank-tensorial property that can be used to test for the presence of symmetry elements on the scale of the wavelength of the light. This wavelength, λ, is large with respect to usual lattice constants, a, of non-modulated crystals. The optical activity is estimated to have a magnitude in the order of a/λ. The structural periodicities that are present in incommensurately modulated crystals, however, are much larger than a. The spatial dispersion is, therefore, not necessarily weak. Thus, a relatively large optical activity might result, under the condition that it is allowed by symmetry. It was shown by Meekes and Janner [15] that one can take the large structural periodicities into account by considering also $\boldsymbol{k} \neq 0$ Fourier components of both dielectric and gyration tensors. Moreover, the symmetry restrictions imposed by the superspace group were evaluated by these authors. It was found that the gyration tensor can have non-vanishing elements for a centrosymmetric superspace group, whereas the point group of the average structure, and also the point group of the superspace group do not allow for non-zero gyration tensor elements [16, 15]. In the case of $((CH_3)_4N)_2ZnCl_4$ we could not detect any non-zero gyration, or any other effect caused by a symmetry breaking due to the modulation [14]. In this paper, we pursue the search for the influence of the incommensurate modulation on optical properties for the case of $((CH_3)_4N)_2CuCl_4$. *This material is interesting for several reasons.*

The crystals of $((CH_3)_4N)_2CuCl_4$ have an orange colour due to the absorption edge at $\lambda \approx 500$ nm. The position of this edge depends (weakly) on the temperature and shows characteristic behaviour at the phase transitions [17]. By means of band structure calculations [18] it was found that the $[CuCl_4]^{2-}$ tetrahedra play the dominant role in the formation of the absorption band. It is well known that the modulation influences the orientations of these tetrahedra in $((CH_3)_4N)_2MCl_4$ (M = Zn, Fe, Co, Ni, and Mn) crystals. *We want to point out that there is an important Jahn–Teller distortion [2] in the M = Cu* compound. It is interesting, therefore, to investigate the influence of the modulation on the dichroic optical properties. We report on measurements of both the linear and the circular dichroism of $((CH_3)_4N)_2CuCl_4$. The latter effect is forbidden by symmetry in centrosymmetric media, in the same way as optical activity is. Furthermore, it is well

known that refractive indices n can increase considerably at an absorption edge [19]. The wavelength of the light in the crystal, $\lambda = \lambda_0/n$, is then considerably reduced (λ_0 is the wavelength of the light in vacuum). This leads to an increase of the optical activity, because the size of the effect behaves as a/λ. It is interesting, therefore, to measure optical activity in incommensurately modulated crystals, with an average centrosymmetric structure, using wavelengths near an absorption edge. In this paper we report on such measurements. The compound $((CH_3)_4N)_2CuCl_4$ is further interesting because it has a monoclinic and centrosymmetric lock-in phase. The optical activity is, therefore, necessarily zero in this phase. On the other hand, the optical indicatrix can rotate around the unique axis of the monoclinic structure. Therefore, it is interesting to search for an indicatrix rotation already in the incommensurate phase. Such a rotation is forbidden if the incommensurate phase has the orthorhombic symmetry of the average structure.

The simultaneous measurement of linear birefringence, linear dichroism, circular birefringence (i.e. optical activity), circular dichroism and indicatrix rotation is by no means straightforward. It can be accomplished with the High Accuracy Universal Polarimeter (HAUP). This instrument was introduced by Kobayashi and Uesu [20] for the simultaneous measurement of linear birefringence, optical activity and indicatrix rotation. Recently, we have shown [21] how HAUP can be used for absorbing and magnetic crystals, so that dichroic effects can also be measured.

The HAUP technique has already been used for the investigation of $((CH_3)_4N)_2CuCl_4$. In these investigations the wavelength $\lambda = 632.8$ nm was used, which is above the absorption edge. The dichroic effects are then negligible. The first HAUP measurements on $((CH_3)_4N)_2CuCl_4$ were reported by Uesu and Kobayashi [22]. At the phase transition from the incommensurate to the lock-in phase a large thermal hysteresis (about 7 K) was observed in the results for the gyration tensor element g_{13} (for the settings used in this paper). The measured gyration was clearly non-zero only in the incommensurate phase. The thermal hysteresis was also detected in the linear birefringence of the sample. Sawada *et al* [4] observed a thermal hysteresis of about 10 K at the same phase transition in measurements of the dielectric constant. The cause of such a hysteresis is often found in the role played by defects (see for example Hamano *et al* [23]). The width of the hysteresis can therefore be used as an indication of the quality of $((CH_3)_4N)_2CuCl_4$ crystals. It is clear that HAUP measurements on a $((CH_3)_4N)_2CuCl_4$ sample with a smaller thermal hysteresis are desirable. In this paper we report on such measurements.

The HAUP measurements of Uesu and Kobayashi [22] showed, in addition, a rotation of the optical indicatrix in the incommensurate phase around the axis that is the unique axis in the first commensurate lock-in phase. Both the observation of a non-zero gyration and the rotation of the indicatrix imply that the point group symmetry of the incommensurate phase cannot be *mmm*. The measurement of g_{13} was later repeated by Saito *et al* [24] and again a clearly non-zero result was obtained in the incommensurate phase. In this paper we also report on measurements of the gyration g_{13} of $((CH_3)_4N)_2CuCl_4$ for the same wavelength $\lambda = 632.8$ nm as used by Uesu and Kobayashi [22]. We wanted to repeat these measurements, because, contrary to the group of Kobayashi, we found that optical activity was too small to be detected in the case of $((CH_3)_4N)_2ZnCl_4$ (see Kremers *et al* [14]). For that case a controversy still exists.

Ortega *et al* [12] also performed HAUP measurements on $((CH_3)_4N)_2CuCl_4$ crystals. These authors measured the gyration tensor element g_{33}. The direction of light propagation is then parallel to the modulation wave vector. The gyration in the incommensurate phase was found to be smaller than the experimental error. The rotation of the optical indicatrix was not studied by these authors. Their measurements were performed at the wavelength

$\lambda = 632.8$ nm, where dichroic effects can be neglected. We report on HAUP measurements of the gyration tensor element g_{33} both for that wavelength and for a wavelength near the absorption edge. Moreover, the rotation of the optical indicatrix and dichroic effects are studied.

This paper is organized in the following way. First, we describe the crystal structure for the successive phases of $((CH_3)_4N)_2CuCl_4$ in order to clarify the optical effects that can be expected. Then, the sample preparation is treated and the most important details of the measuring method are given. Subsequently, the interpretation of the measurements is discussed, because this is an essential part of the HAUP technique. After this, we present the results obtained, which are then discussed.

2. The crystal structure of $((CH_3)_4N)_2CuCl_4$ as a function of temperature

The four successive phases that occur in $((CH_3)_4N)_2CuCl_4$ upon changing the temperature are characterized in table 1. The temperatures T_i and T_{c1} are those that we observe in our measurements. The value $T_i = 299$ K agrees with that of Ortega *et al* [12], though it is often claimed that $T_i = 297$ K. The high-temperature paraelastic phase (I) is centrosymmetric and orthorhombic ($|a| = 15.155$ Å, $|b| = 9.039$ Å and the pseudo-hexagonal axis $|c| = 12.127$ Å). The gyration tensor is, therefore, necessarily zero and the indicatrix has a fixed orientation. The HAUP measurements in the paraelastic phase can, therefore, be used as a reference for the results in the incommensurate phase (II) and the lock-in phase (III).

Table 1. Successive phase transitions in $((CH_3)_4N)_2CuCl_4$. The parameter γ determines the modulation wave vector according to the relation $q = \gamma c^*$. It is important to note that the superspace group symmetry of the incommensurate phase has not been checked experimentally. The indicatrix rotation is given with respect to the orthorhombic structure of the paraelastic phase I.

Phase	IV	III	II	I
Temperature (K)	<263 ($= T_{c2}$)	<292.4 ($= T_c$)	<299 ($= T_i$)	>299 ($= T_i$)
Symmetry	$P112_1/n$	$P2_1/c11$	$Pcmn(00\gamma)(1s\bar{1})$?	$Pcmn$
γ	0	2/3	$(2+\delta)/3$	0
Type	Ferroelastic	Ferroelastic	Incommensurate	Paraelastic
Domain walls	(100)	(001)		
System	Monoclinic	Monoclinic	Orthorhombic?	Orthorhombic
Gyration tensor g	0	0	?	0
Indicatrix rotation	Around c	Around a	?	None

Vlokh *et al* [17] showed by means of precise birefringence measurements that the modulation wave vector q shows some variation with temperature in the incommensurate phase (II). In the same paper, the authors showed that there is a large influence of (x-ray-induced) defects on both the temperature behaviour of the modulation wave vector and on the value of T_c. The lock-in phase transition temperature T_c increases with the defect concentration. Therefore, one can state that the temperature width of the incommensurate phase is an indication of the quality of the crystal.

Below T_c the modulation wave vector of $((CH_3)_4N)_2CuCl_4$ locks in at $q = \frac{2}{3}c^*$. The crystal then has a threefold superstructure. Ferroelastic domains are formed in this monoclinic lock-in phase with twin planes parallel to (001) [4]. The indicatrix can rotate up to approximately 4×10^{-2} rad around the a axis in a single domain [5]. Although each of

the domains is centrosymmetric it is still expected that the multi-domain state of the sample is optically active [25, 26].

A third phase transition takes place at $T_{c2} = 263$ K [5]. The value of γ becomes zero and the structure is monoclinic with the c axis as unique axis. The twin planes between the domains are parallel to (100). Again, each domain is centrosymmetric, but a multi-domain sample is expected to be optically active.

3. The samples

The growth of good quality crystals is more difficult for $((CH_3)_4N)_2CuCl_4$ than for the related compound $((CH_3)_4N)_2ZnCl_4$. We have grown $((CH_3)_4N)_2CuCl_4$ crystals by the thermal convection method as described by Arend *et al* [27]. The stoichiometric solution of $((CH_3)_4N)Cl$ and $CuCl_2$ in water has a dark green colour. If the thermal convection is too large, one can easily observe many solution inclusions in the orange crystals. According to our experience, nicely faceted, inclusion-free crystals of about 0.5 cm^3 can be grown in several months if a small thermal convection is used ($\Delta T = 1.5$ K). With an optical goniometer it is easy to identify the natural crystal faces. The as-grown $((CH_3)_4N)_2CuCl_4$ crystals are often platelike with large (001) faces or they are extended along the *c*-direction and have large (110) and (1$\bar{1}$0) faces. The (010) faces are usually very small, contrary to the (100) faces.

From these crystals we have cut, with a wire saw, two platelets. One was parallel to the natural (001) face and the other was parallel to the (101) face. Both sides of these plates were polished on felt with diamond paste down to $\frac{1}{4}$ μm size. It was checked with a polarizing microscope that both polished faces of each sample were plane-parallel. Due to the large linear birefringence one observes thickness changes of the sample as a change in colour of the transmitted light. Within the spot of the light beam the variation in thickness is less than 5 μm.

Table 2. The two samples of $((CH_3)_4N)_2CuCl_4$ used in the present experiments. n_a, n_b and n_c are the main refractive indices of the crystal. g is the gyration tensor and s is the unit wave vector of the incident light with respect to the crystallographic axes of the paraelastic phase.

Sample	Sample surface	Thickness z (mm)	Linear birefringence Δn	Gyration $G(s) = g_{ij}s_is_j$
1	(001)	0.14	$\Delta n_{33} = n_b - n_a$	$G_{33} = g_{33}$
2	(101)	0.22	$\Delta n_{13} \approx 0.61(n_b - n_a) + 0.39(n_c - n_b)$	$G_{13} = 0.39g_{11} + 0.61g_{33} + 0.98g_{13}$

The linear birefringence and gyration of the two samples are given in table 2.

4. Measurements

All measurements have been performed with the HAUP apparatus built in our laboratory as described by Dijkstra *et al* [28]. This original version of the apparatus appeared to be inadequate for performing reliable measurements and some essential improvements were, therefore, carried out [29].

In table 3 an overview is given of the measurements that have been performed on the two samples. There were two reasons for performing the wavelength-dependent HAUP measurements. As explained in the introduction, it is interesting to measure the optical

properties of an incommensurately modulated crystal near an absorption edge as a function of temperature. The measurement as a function of the wavelength reveals the position of the absorption edge. In this way we found that $\lambda \approx 511$ nm is a good choice for the HAUP measurement near the absorption edge. Moreover, the value of the linear birefringence must be known at a certain combination of temperature and wavelength that is used in the measurement. This is necessary for the determination of the behaviour of the linear birefringence with changing temperature or wavelength. The temperature dependences of the linear birefringences Δn_{13} and Δn_{33} for the wavelength $\lambda = 632.8$ nm were given by, respectively, Saito *et al* [24] and Ortega *et al* [12]. Using these values, the linear birefringences as a function of wavelength were derived at a constant temperature from the wavelength-dependent HAUP measurement. Subsequently, the linear birefringence could be determined for the HAUP measurement at the wavelength $\lambda = 511$ nm.

Table 3. Specification of the three HAUP measurements that have been performed on each of the two samples.

Sample	Measurement I: λ-dependence	Measurement II: T-dependence	Measurement III: T-dependence
(001)	$T = 296$ K	$\lambda = 632.8$ nm	$\lambda = 511$ nm
(101)	$T = 296.8$ K	$\lambda = 632.8$ nm	$\lambda = 511$ nm

At least two extinction directions [29] were measured in each of the performed HAUP experiments. This is necessary for the separation of circular dichroism from indicatrix rotation (see also Kremers and Meekes [21]). Both of these effects are of interest. The temperature was left to stabilize for about half an hour after each change of its value. In case of shorter stabilization times it was sometimes observed that, for example, the optical activity showed a definite change with temperature in the paraelastic phase. Optical activity is, however, symmetry forbidden in this phase. After a temperature stabilization of about half an hour the results of the measurements were as expected.

5. Interpretation of the measurements

In a HAUP experiment first the position Θ_0 of an extinction direction is determined with respect to an arbitrary, but fixed, origin. In our case, we rotate both polarizers to a position of minimal intensity, while keeping them crossed. Subsequently, intensities are measured at different polarizer positions. The angle Θ of the polarizer, measured with respect to Θ_0, is kept within 2×10^{-2} rad. Also the angle Y of the analyser, measured with respect to the crossed polarizers position, is kept within the same small range. This allows for the fitting of the measured intensities to the so-called HAUP intensity formula. Recently, we have derived a unified formula for absorbing crystals [21]. For the case that we consider here this formula reduces to:

$$\Gamma/\Gamma_0 = \exp\left(-2\tilde{\kappa}\frac{2\pi z}{\lambda}\right)\begin{pmatrix} 1 & Y & Y^2 \end{pmatrix} C^{\Theta_0}_{(3\times 3)} \begin{pmatrix} 1 \\ \Theta \\ \Theta^2 \end{pmatrix} \tag{1}$$

with

$$
\begin{aligned}
C_{21}^{\Theta_0} &= -(2k+(p-a))\sin\left(\frac{2\pi z}{\lambda}\Delta n\right)+2\delta Y\cos^2\left(\frac{\pi z}{\lambda}\Delta n\right)\\
&\quad+\frac{2\pi z}{\lambda}\Delta\kappa(p+a)\cot\left(\frac{\pi z}{\lambda}\Delta n\right)\\
C_{12}^{\Theta_0} &= 0\\
C_{22}^{\Theta_0} &= 2\exp\left(\frac{2\pi z}{\lambda}\Delta\kappa\right)-2\cos\left(\frac{2\pi z}{\lambda}\Delta n\right)\\
C_{31}^{\Theta_0} &= \exp\left(\frac{2\pi z}{\lambda}\Delta\kappa\right)\\
C_{13}^{\Theta_0} &= 2\left(\cosh\left(\frac{2\pi z}{\lambda}\Delta\kappa\right)-\cos\left(\frac{2\pi z}{\lambda}\Delta n\right)\right)
\end{aligned}
\tag{2}
$$

and z is the thickness of the sample platelet. All other coefficients $C_{ij}^{\Theta_0}$ are zero, except $C_{11}^{\Theta_0}$. This term has not been worked out specifically, because it is not used to extract optical parameters from the measurement. The expression for Θ_0, defining the position of the extinction direction, is

$$\Theta_0 = -\frac{1}{2}\delta Y+\frac{1}{2}(p+a)\cot\left(\frac{2\pi z}{\lambda}\Delta n\right)-k'+\delta\Theta_{\text{indicatrix}}. \tag{3}$$

Here, $\Delta n = n_1 - n_2$ is the *linear birefringence* and $\Delta\kappa = \kappa_1 - \kappa_2$ is the *linear dichroism*. The *circular birefringence* $n_r - n_l$ is related to the parameter k:

$$k = \frac{n_r - n_l}{2\,\Delta n} \tag{4}$$

and the *circular dichroism* $\kappa_r - \kappa_l$ is related to k':

$$k' = \frac{\kappa_r - \kappa_l}{2\,\Delta n}. \tag{5}$$

The gyration G and the circular birefringence are related in the following way:

$$n_r - n_l = \frac{G}{\tilde{n}} \tag{6}$$

where $\tilde{n}$ is the average of the two refractive indices n_1 and n_2 that determine the linear birefringence. In the same way, $\tilde{\kappa}$ in equation (1) is the average of the two extinction coefficients κ_1 and κ_2 that determine the linear dichroism. The parameter $\delta\Theta_{\text{indicatrix}}$ in equation (3) describes the rotation of the optical indicatrix. Note that in the expressions for $C_{21}^{\Theta_0}$ and Θ_0 the linear dichroism has been considered to be small with respect to the linear birefringence.

In the fit of the intensities to the HAUP intensity formula both the so-called ΔY-correction and the $\Delta\Theta$-correction are performed [29]. By means of the ΔY-correction the contribution of the systematic error δY is reduced to a large extent. The $\Delta\Theta$-correction improves the values of all fitting parameters C_{ij} and gives a correction to the value of Θ_0.

Besides δY two other systematic errors, p and a, must be extracted from the fitting parameters in order to determine the circular birefringence, the circular dichroism and the indicatrix rotation. The linear birefringence and the linear dichroism can be calculated without a knowledge of the systematic errors. The errors p and a describe the parasitic ellipticities of the light polarized by, respectively, the polarizer and the analyser. In short, the systematic errors are extracted by studying the fitting parameters as a function of temperature

(or wavelength) in a region of small linear dichroism where there is no circular birefringence, no circular dichroism and no indicatrix rotation. In the case of $((CH_3)_4N)_2CuCl_4$ we use for this the orthorhombic and centrosymmetric paraelastic phase. The value of δY is found as the slope of a straight line fitted to a plot of $C_{21}^{\Theta_0}/\sin((2\pi z/\lambda)\Delta n)$ against $\cot((\pi z/\lambda)\Delta n)$. The value of $p+a$ is obtained in the same way by plotting Θ_0 against $\cot((\pi z/\lambda)\Delta n)$. We take the value of $p-a$ such that the average value of k becomes zero in the centrosymmetric paraelastic phase. If the systematic errors are known, one can calculate the optical properties of the sample from the fitting parameters. For a detailed description of the procedure used we refer to Kremers and Meekes [21, 29].

6. Results

6.1. Sample quality

All temperature-dependent measurements were performed by cooling down from the paraelastic phase (I) to the lock-in phase (III). For the (101) sample and the wavelength $\lambda = 632.8$ nm we subsequently performed an additional measurement by increasing the temperature. The corresponding behaviour of the fitting parameter C_{21} is plotted in figure 1. It shows a sharp change at the phase transition temperature $T_c = 292.4$ K. The thermal hysteresis (about 0.6 K) at this phase transition is very small with respect to the value of 10 K sometimes observed. Moreover, the temperature width of the incommensurate phase, here 6.6 K, is as can be expected for a crystal with a very low defect concentration [17]. We conclude, therefore, that our $((CH_3)_4N)_2CuCl_4$ crystals are of very good quality.

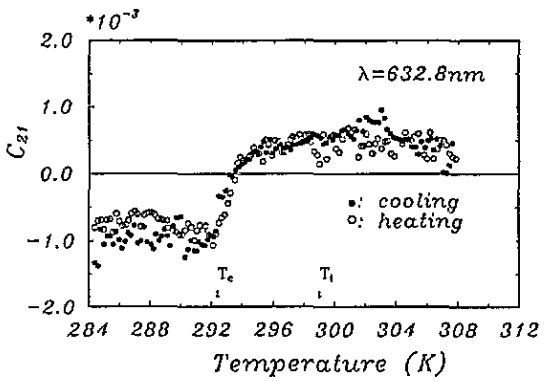

Figure 1. The fitting parameter C_{21} for the (101) sample and a wavelength $\lambda = 632.8$ nm. A very small thermal hysteresis is observed at T_c. The values of T_i and T_c have been derived from the results for the linear birefringence, which are presented further on.

6.2. The linear birefringence Δn_{33} and the linear dichroism $\Delta\kappa_{33}$

In figure 2 the linear birefringence Δn_{33} is shown as found for the wavelength $\lambda = 632.8$ nm. There is a reasonable agreement with the results of Ortega *et al* [12], although our values are about 2% lower. This may be caused by an inaccurate measurement of the sample thickness. In order to derive the linear birefringence from a HAUP experiment it is necessary to know its value for a single value of the parameter (e.g. temperature, wavelength) that is varied during the measurement.

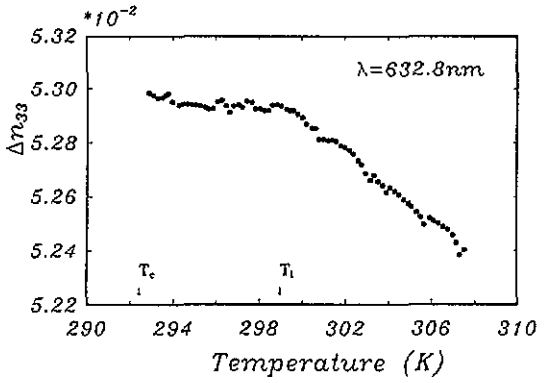

Figure 2. The linear birefringence Δn_{33} as a function of temperature in the paraelastic and incommensurate phase of $((CH_3)_4N)_2CuCl_4$. The wavelength of the light is $\lambda = 632.8$ nm.

The result of figure 2 has been used, therefore, to derive the wavelength dependence of the linear birefringence at the temperature $T = 296$ K from the corresponding HAUP measurement. The results are given in figure 3. Thus, it can be seen by extrapolation that the value of Δn_{33} ($T = 296$ K, $\lambda = 632.8$ nm) agrees with the results of figures 2 and 3.

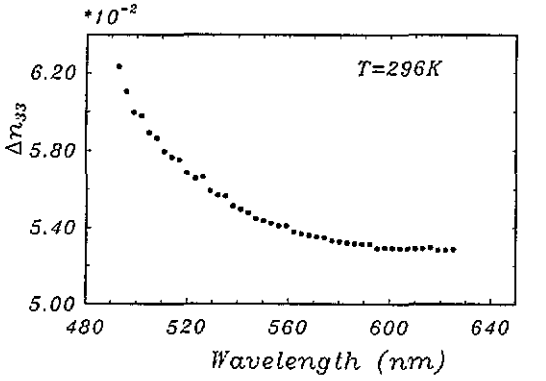

Figure 3. The linear birefringence Δn_{33} of $((CH_3)_4N)_2CuCl_4$ as a function of the wavelength λ of the light at the temperature $T = 296$ K. The discontinuities in this figure are a result of the fact that HAUP gives inaccurate results whenever $\sin((\pi z/\lambda)\Delta n) = 0$.

The temperature dependence of the linear birefringence at a wavelength $\lambda = 511$ nm is given in figure 4. This has been done in such a way that it gives the best agreement with the data in figure 3 at $\lambda = 511$ nm. Both phase transitions at T_i and T_c can clearly be observed. The linear birefringence Δn_{33} shows a discontinuity at $T_c = 292.4$ K. It is interesting to see that the linear birefringence has a smoother behaviour in the paraelastic phase for the measurements in figure 4 than those in figure 2, although both figures are for the same sample. This difference may be related to the thermal history of the sample. The choice for the measurement at the wavelength $\lambda = 511$ nm was made by considering the wavelength dependence of the linear dichroism, which is presented in figure 5. For wavelengths larger than 570 nm the linear dichroism $\Delta\kappa_{33}$ is negligible. The linear dichroism shows a sharp increase at the absorption edge. It was impossible to measure at wavelengths smaller than $\lambda = 490$ nm, because the light was absorbed too strongly there. At $\lambda = 511$ nm the

linear dichroism is clearly non-zero. On the other hand it is still small with respect to the linear birefringence. Therefore, the HAUP intensity formula (2) can be used for the interpretation of the measurements. It was explained in the introduction that the temperature dependence of the linear dichroism $\Delta\kappa_{33}$ for such a wavelength near the absorption edge could be sensitive to the incommensurate modulation. The result is shown in figure 6. Unfortunately, only a linear decrease of $\Delta\kappa_{33}$ is seen with decreasing temperature. Even at the phase transition temperatures T_i and T_c no structure is observed. The sign of $\Delta\kappa_{33}$ is different in figure 6 than in figure 5. This is caused by the fact that the, arbitrarily chosen, first extinction direction differed by $\frac{1}{2}\pi$ between these measurements.

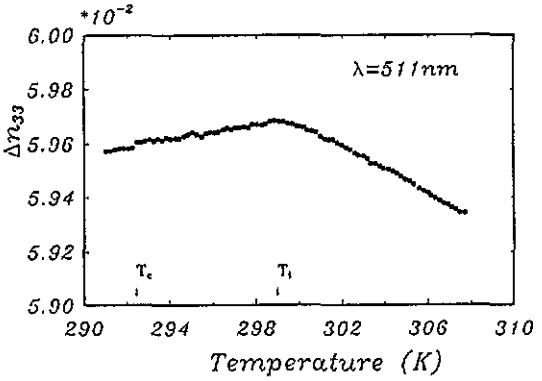

Figure 4. The linear birefringence Δn_{33} of $((CH_3)_4N)_2CuCl_4$ as a function of temperature in the paraelastic, in the incommensurate and (partly) in the first lock-in phase of $((CH_3)_4N)_2CuCl_4$. The wavelength of the light is 511 nm.

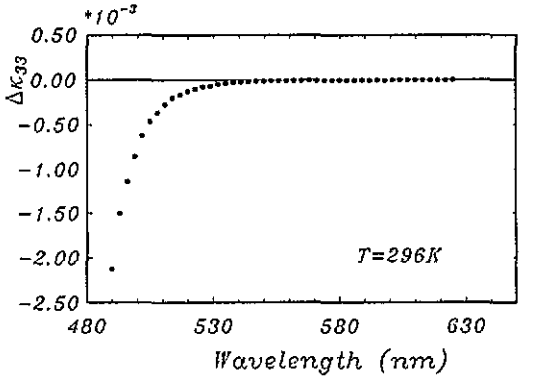

Figure 5. The linear dichroism $\Delta\kappa_{33}$ of $((CH_3)_4N)_2CuCl_4$ as a function of the wavelength λ of the light. The temperature is $T = 296$ K.

6.3. The linear birefringence Δn_{13} and the linear dichroism $\Delta\kappa_{13}$

In the figures 7 and 8 we show the temperature dependence of the linear birefringence Δn_{13} at, respectively, $\lambda = 632.8$ nm and $\lambda = 511$ nm. Both are in good agreement with the wavelength dependence of the linear birefringence Δn_{13}, which is presented in figure 9, at the temperature $T = 296.8$ K. The temperature dependence of Δn_{13} is in reasonable

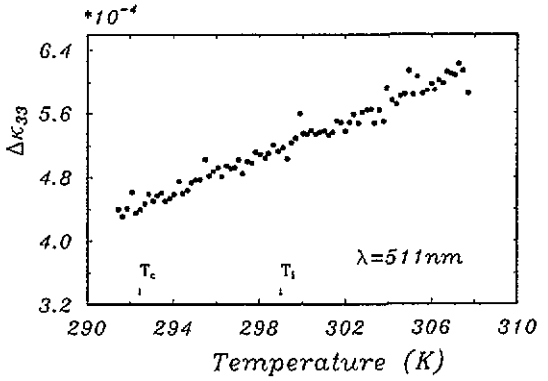

Figure 6. The linear dichroism $\Delta\kappa_{33}$ of $((CH_3)_4N)_2CuCl_4$ as a function of the temperature. The wavelength of the light is $\lambda = 511$ nm.

agreement with the results of Saito *et al* [24], although our values are, also for this case, about 2% lower. It is interesting that at $T \approx 305$ K a clear change in slope is observed for both wavelengths used. The reason for this change is unclear to us. Moreover, the linear birefringences Δn_{33} in figures 2 and 4 do not show a change of slope at this temperature.

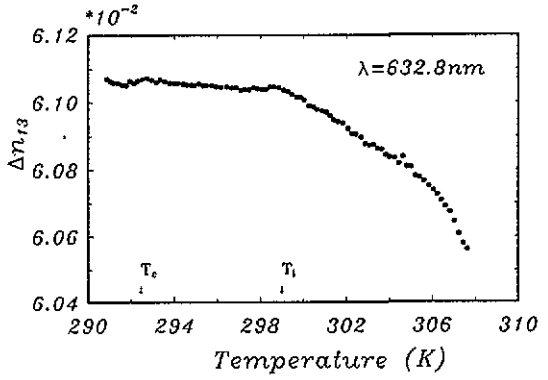

Figure 7. The linear birefringence Δn_{13} of $((CH_3)_4N)_2CuCl_4$ as a function of temperature in the paraelastic, in the incommensurate and (partly) in the first lock-in phase of $((CH_3)_4N)_2CuCl_4$. The wavelength of the light is $\lambda = 632.8$ nm.

In figure 10 we present the wavelength dependence of the linear dichroism $\Delta\kappa_{13}$ at the temperature $T = 296.8$ K. Again, it is seen that at $\lambda = 511$ nm a clearly non-zero linear dichroism is present that is still small with respect to the linear birefringence. The result for the temperature dependence of the linear dichroism $\Delta\kappa_{13}$ at this wavelength is plotted in figure 11. Also in this case, only a linear dependence on temperature is observed with no structure at the phase transitions. The temperature dependence of $\Delta\kappa_{33}$ is larger than that of $\Delta\kappa_{13}$.

6.4. Optical activity

As expressed by equation (4), the circular birefringence $n_r - n_l$ is determined by the ellipticity k and the linear birefringence. In figures 12 and 13 the temperature dependence of k is presented for the (001) sample.

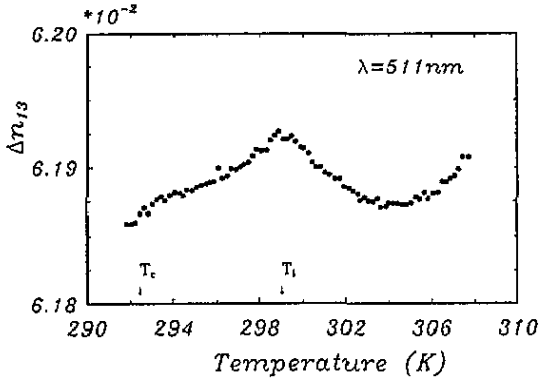

Figure 8. The linear birefringence Δn_{13} of $((CH_3)_4N)_2CuCl_4$ as a function of temperature in the paraelastic, in the incommensurate and (partly) in the first lock-in phase of $((CH_3)_4N)_2CuCl_4$. The wavelength of the light is 511 nm.

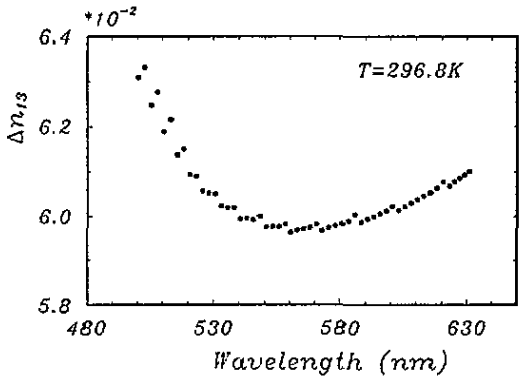

Figure 9. The linear birefringence Δn_{13} of $((CH_3)_4N)_2CuCl_4$ as a function of the wavelength λ of the light at the temperature $T = 296.8$ K.

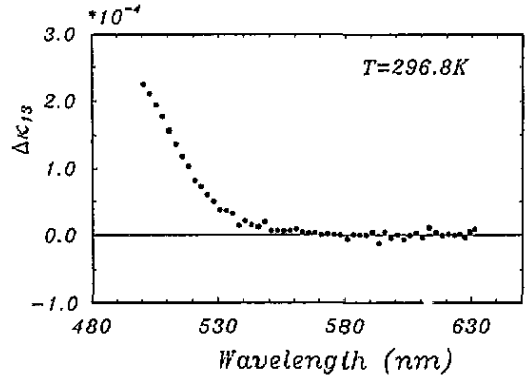

Figure 10. The linear dichroism $\Delta\kappa_{13}$ of $((CH_3)_4N)_2CuCl_4$ as a function of the wavelength λ of the light. The temperature is $T = 296.8$ K.

In the case of the measurement with $\lambda = 632.8$ nm, figure 12, we observe that $|k| < 1.5 \times 10^{-4}$ for the majority of points. Moreover, the results scatter around zero

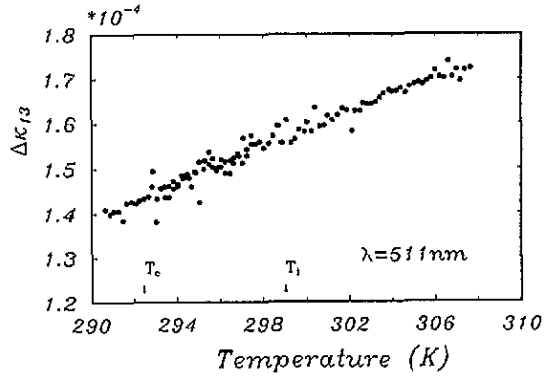

Figure 11. The linear dichroism $\Delta\kappa_{13}$ of $((CH_3)_4N)_2CuCl_4$ as a function of the temperature. The wavelength of the light is $\lambda = 511$ nm.

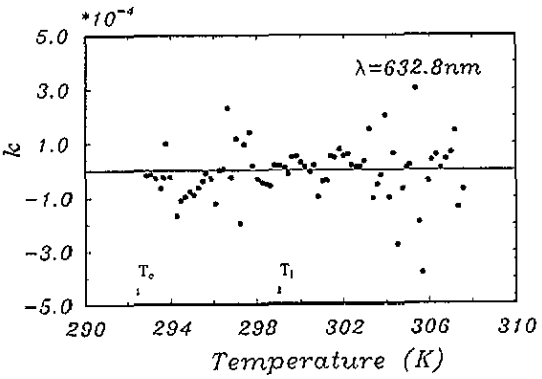

Figure 12. The ellipticity $k = (n_r - n_l)/(2\,\Delta n)$ for the (001) sample of $((CH_3)_4N)_2CuCl_4$ as a function of temperature. The wavelength of the light is $\lambda = 632.8$ nm.

in both the paraelastic and the incommensurate phase. These results agree with those of Ortega *et al* [12]. We have to conclude that the gyration G_{33} in the incommensurate phase is zero or too small to be detected at the wavelength $\lambda = 632.8$ nm. It has been explained in the introduction, though, that optical activity, if present, may be more pronounced for wavelengths near the absorption edge. The results for the corresponding measurement using $\lambda = 511$ nm, figure 13, show that $|k| < 1 \times 10^{-4}$ for nearly all points. It is, therefore, not possible to detect optical activity G_{33} in the incommensurate phase, not even for this wavelength.

Nevertheless, a non-zero gyration G_{13}, measured with HAUP, has been reported by Uesu and Kobayashi [22] and Saito *et al* [24]. In figure 14 we show our results for the same wavelength, $\lambda = 632.8$ nm, as used by these authors. In general, the value of $|k|$ is smaller than 1×10^{-4} for temperatures higher than $T = 295$ K. Nevertheless, a systematic deviation from zero is observed. Below $T = 295$ K a clear onset of the gyration G_{13} is observed. Moreover, the ferroelastic phase III shows a large gyration, $k \approx -8 \times 10^{-4}$, though this phase is centrosymmetric. In our opinion, this effect is inevitable, because the sample enters a multi-domain state. The gyration is a result of the change in orientation of the optical indicatrix from one domain to the next. Our results are clearly different from those obtained by Uesu and Kobayashi [22] and Saito *et al* [24]. This difference is

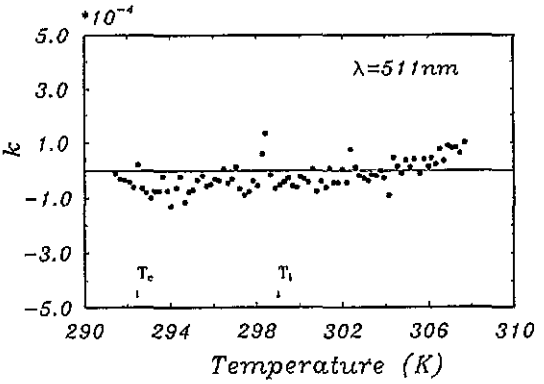

Figure 13. The ellipticity $k = (n_r - n_l)/(2\,\Delta n)$ for the (001) sample of $((CH_3)_4N)_2CuCl_4$ as a function of temperature. The wavelength of the light is $\lambda = 511$ nm.

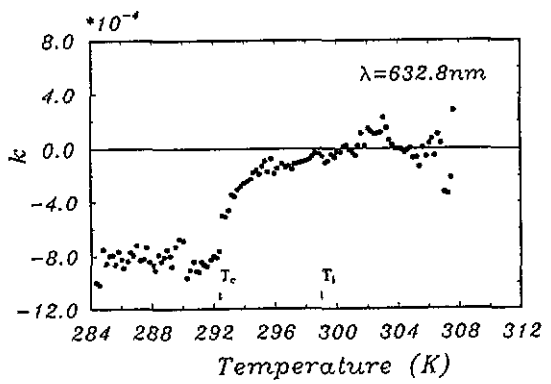

Figure 14. The ellipticity $k = (n_r - n_l)/(2\,\Delta n)$ for the (101) sample of $((CH_3)_4N)_2CuCl_4$ as a function of temperature. The wavelength of the light is $\lambda = 632.8$ nm.

addressed in the discussion.

The ellipticity k at the wavelength $\lambda = 511$ nm near the absorption edge for the same (101) sample has been plotted in figure 15. The open circles are the results obtained for a measurement with a stabilization time of only 15 minutes at each temperature. The ellipticity k is, then, not even constant in the centrosymmetric paraelastic phase. Therefore, we have used a stabilization time of about 30 minutes for all temperature-dependent measurements. The results thus obtained are represented by the full circles. Again, it is observed that at a temperature $T = 295$ K there is an onset of gyration G_{13} in the incommensurate phase.

6.5. The circular dichroism and indicatrix rotation

In order to calculate the circular dichroism and the indicatrix rotation one must measure two extinction directions. After the determination of the systematic errors separately for both extinction directions and the linear birefringence one subtracts the contribution $-\frac{1}{2}\delta Y + \frac{1}{2}(p + a)\cot((\pi z/\lambda)\Delta n)$ from the measured values of Θ_0. In addition, $\frac{1}{2}\pi$ is subtracted from Θ_0 for the second extinction direction. The resulting values are plotted in figure 16 for the temperature-dependent measurement of the (001) sample at the wavelength $\lambda = 511$ nm.

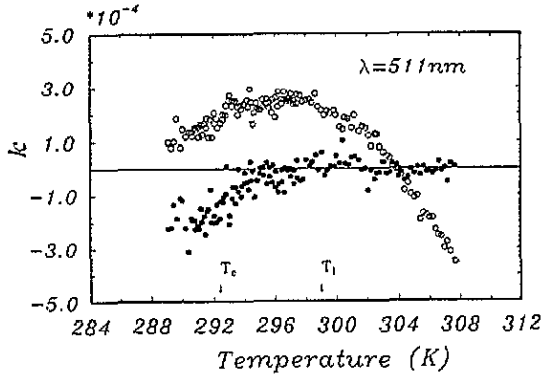

Figure 15. The ellipticity $k = (n_r - n_l)/(2\,\Delta n)$ for the (101) sample of $((CH_3)_4N)_2CuCl_4$ as a function of temperature. The wavelength of the light is $\lambda = 511$ nm. The open circles give the result with a temperature stabilization of 15 minutes. The full circles represent the results obtained with a stabilization time of 30 minutes.

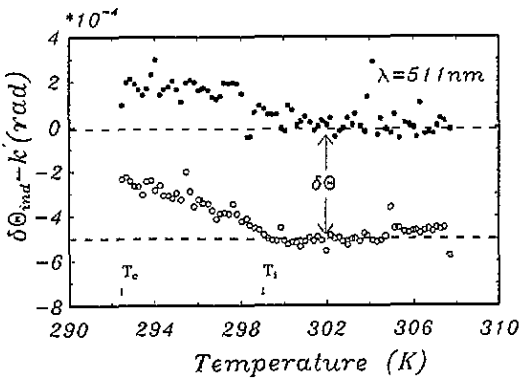

Figure 16. The values of $\delta\Theta_{ind} - k'$ for the two extinction directions as obtained for the measurement on the (001) sample. The wavelength of the light is $\lambda = 511$ nm.

The paraelastic phase is orthorhombic and centrosymmetric. Therefore, there can be no indicatrix rotation and no circular dichroism in this phase. The curves in figure 16 should coincide, therefore. Nevertheless, there is a difference caused by the so-called $\delta\Theta$-error [21]. For this measurement $\delta\Theta = 5.57 \times 10^{-4}$ rad.

Both curves in figure 16 show the expected constant behaviour in the paraelastic phase. At T_i, however, there is a deviation from this behaviour. This can be caused by both circular dichroism and indicatrix rotation. These effects can, however, be separated, because the circular dichroism has different signs for both extinction directions, whereas the indicatrix rotation has equal signs [21].

In figure 17 we present the values of the indicatrix rotation $\delta\Theta_{indicatrix}$ thus obtained. There is no absolute scale on the ordinate axis, because the Θ_0-values are measured with respect to an arbitrary origin. Nevertheless, a definite rotation of the optical indicatrix is observed in the incommensurate phase with a maximum of about 2×10^{-4} rad.

The circular dichroism is obtained by taking the difference of the two curves in figure 16 and multiplying the result with $2\,\Delta n$ according to equation (5). The values thus obtained are plotted in figure 18. It is seen that, with respect to the experimental error, there is no

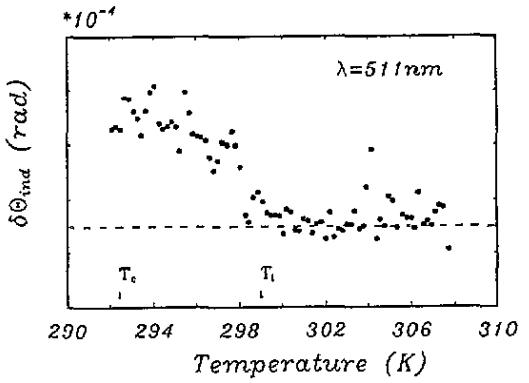

Figure 17. Rotation of the optical indicatrix in the (001) sample for the wavelength $\lambda = 511$ nm. The distance between tick marks on the ordinate axis equals 1×10^{-4}. There is no absolute scale, because Θ_0 can only be measured with respect to an arbitrary origin.

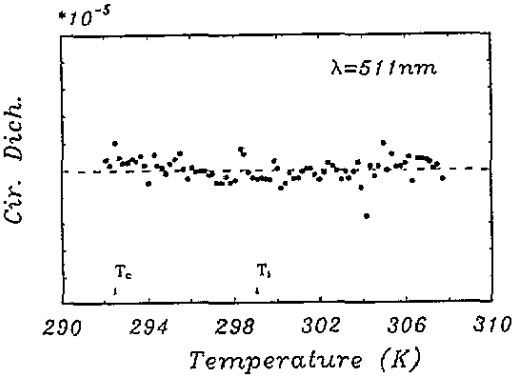

Figure 18. The circular dichroism $\kappa_r - \kappa_l$ of the (001) sample for the wavelength $\lambda = 511$ nm. The distance between tick marks on the ordinate axis equals 1×10^{-5}.

detectable circular dichroism in the incommensurate phase. The same conclusion had to be drawn for all other measurements. A rotation of the indicatrix, however, was observed in all cases, having the same order of magnitude. We have plotted the corresponding results in the figures 19 and 20. The result for the (101) sample at the wavelength $\lambda = 632.8$ nm has been plotted in figure 21. The change in indicatrix rotation is larger as compared to the case of the (001) sample and the scatter of data points is smaller. Striking, however, is the increase in scatter at temperatures well above the phase transitions and the fact that the value of $\delta\Theta_{\text{indicatrix}}$ is not constant in the paraelastic phase. The reason for this is, at present, unclear to us.

7. Discussion and conclusions

The measurements in this paper have been performed in order to search for optical effects in the incommensurate phase of $((CH_3)_4N)_2CuCl_4$ that are not allowed by the symmetry of the average structure. The temperature dependence of the optical effects has been studied for $\lambda = 632.8$ nm and $\lambda = 511$ nm. The latter wavelength is near the absorption edge. A sample platelet parallel to (001) and one parallel to (101) have been used for the investigations. We

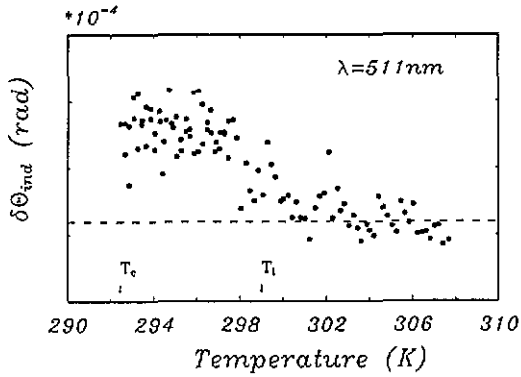

Figure 19. Rotation of the optical indicatrix in the (101) sample for the wavelength $\lambda = 511$ nm. The distance between tick marks on the ordinate axis equals 1×10^{-4}.

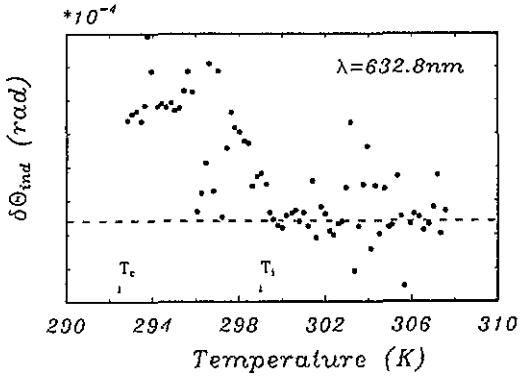

Figure 20. Rotation of the optical indicatrix in the (001) sample for the wavelength $\lambda = 632.8$ nm. The distance between tick marks on the ordinate axis equals 1×10^{-4}.

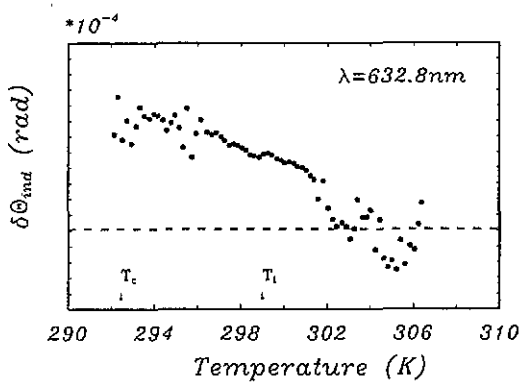

Figure 21. Rotation of the optical indicatrix in the (101) sample for the wavelength $\lambda = 632.8$ nm. The distance between tick marks on the ordinate axis equals 1×10^{-4}.

used the recently extended HAUP method [21]. Also dichroic effects could be measured reliably, therefore, simultaneously with the other effects.

Only a very small thermal hysteresis at T_c was observed in our samples. This, together

with the width of the incommensurate phase, indicates that the samples were of high quality. It has been found that a temperature stabilization time of about 30 minutes is sufficient to give reliable results for all measurements.

The measured values of the linear birefringence were found to be in reasonable agreement with those of other authors. In addition, an unexplained change in the linear birefringence Δn_{13} has been observed at $T \approx 305$ K in the paraelastic phase. The phase transition from this phase to the incommensurate phase is clearly revealed by the linear birefringence. The phase transition temperature that we observed was $T_i = 299$ (± 0.25) K. It is unclear to us why this value disagrees with the often reported value $T_i = 297$ K. The measured linear birefringence showed typical structures in the incommensurate phase. This agrees with the results of Vlokh *et al* [17], who concluded that the modulation wave vector must show a variation with temperature in this phase. The first-order character of the phase transition from the incommensurate to the first ferroelastic lock-in phase showed up as a discontinuity in the linear birefringence at the phase transition temperature.

In advance, it was expected that the influence of the incommensurate modulation on the $[CuCl_4]^{2-}$ tetrahedra would be reflected by the temperature dependence of the linear dichroism $\Delta\kappa$. However, both $\Delta\kappa_{13}$ and $\Delta\kappa_{33}$ only showed a linear dependence on the temperature. Even at the phase transition temperatures the linear dichroism was structureless. Also the circular dichroism was measured, but in all cases it was zero, or too small to be detected.

The measured gyration G_{33} agrees with the results of Ortega *et al* [12] for the wavelength $\lambda = 632.8$ nm. It is zero or too small to be detected. We have checked whether the gyration G_{33}, if non-zero, could be enhanced for a wavelength near an absorption edge, $\lambda = 511$ nm. However, also for this wavelength it was impossible to detect any gyration.

We have also measured the gyration G_{13} at two different wavelengths, because a clearly non-zero G_{13} in the incommensurate phase was reported by Uesu and Kobayashi [22] and Saito *et al* [24]. These authors find a zero gyration in the first lock-in phase. In our measurements, however, a non-zero gyration was found in this phase. We believe that this is a result of the multi-domain state of the sample, which is difficult to avoid without applying external forces. Also the behaviour with temperature of the gyration G_{13} that we measured in the incommensurate phase clearly differs from the results of Uesu and Kobayashi [22] and Saito et al [24]. These authors find a gyration G_{13} that starts deviating from zero below T_i. It becomes maximal halfway to the incommensurate phase and then decreases, until it is zero at T_c. In our case, however, the gyration is very small for temperatures above $T = 295$ K and a steady increase is observed below this temperature. This was found for both wavelengths used. The reason for a non-zero gyration in the incommensurate phase may be found in a symmetry breaking caused by the incommensurate modulation with respect to the average centrosymmetric structure. It is, however, important to realize that a coexistence of commensurate and incommensurate domains is also often observed in the incommensurate phase (see for example Hedoux *et al* [30]). The observed gyration in the incommensurate phase can then be attributed to a steady increase of the number of commensurate domains until only commensurate domains are left at T_c. From our measurements of the linear birefringence, and also those of others (see for example Vlokh *et al* [17]), it is expected that the modulation wave vector modulus is not constant in the incommensurate phase. Unfortunately, the exact behaviour of the modulation wave vector q has not been measured very accurately by means of diffraction experiments. Moreover, the superspace group has not yet been determined experimentally, as far as we know. It is, therefore, not even certain that the average structure of the incommensurate phase is centrosymmetric and orthorhombic. It is clear that a very careful,

temperature-dependent investigation of the incommensurate phase of $((CH_3)_4N)_2CuCl_4$ by means of x-ray or neutron diffraction would be of great help in the interpretation of our results. This may be a topic of further research.

Finally, we discuss the observed rotation of the optical indicatrix in the incommensurate phase that contradicts an orthorhombic symmetry. Contrary to the results of Uesu and Kobayashi [22] we have detected a rotation around the c-axis of about 2×10^{-4} rad in the incommensurate phase. There is no indicatrix rotation in the paraelastic phase. According to the analysis presented by Meekes and Janner [15], a long-wavelength Fourier component of the dielectric tensor with wave vector $\boldsymbol{h} = l\boldsymbol{c}^* + m\boldsymbol{q}$ and l, m both odd, can give rise to such a rotation if the superspace group is $Pcmn(00\gamma)(1s\bar{1})$. In the case where wave vectors $\boldsymbol{h}$ with l even and m odd are also important, a rotation around the a-axis can be expected. Unfortunately, the orientation of our samples was not suited to identifying this rotation. Uesu and Kobayashi [22] did observe a rotation of about 5×10^{-3} rad around the a-axis, but however none around the b- or c-axes. Unfortunately, their sample showed a very large thermal hysteresis, unlike our samples. It is not unlikely that this hysteresis is related to the behaviour of the modulation wave vector influenced by defects. Therefore, we think that it is difficult to compare the results. Nevertheless, their large result might be in correspondence with our results at 632.8 nm that increase from 3.5×10^{-4} rad for the (001) sample to a value of approximately 7×10^{-4} rad observed for the (101) sample. As mentioned before, we have no explanation for the fact that at 632.8 nm the (101) sample shows a non-constant indicatrix rotation in the paraelastic phase.

At present, it is still unclear whether the different results that are obtained by different authors are caused by differences in the (quality) of the samples or by the method of measurement. We would like to suggest, therefore, that a specific set of samples of incommensurately modulated crystals are measured by different groups that work in this field. Moreover, the quality of these samples should be checked by means of additional measurements.

Acknowledgments

We would like to acknowledge Professor Dr P Bennema, Professor Dr T Janssen and Professor Dr A Janner for their support and contributions. This work is part of the research program of the Stichting voor Fundamenteel Onderzoek der Materie (Foundation for Fundamental Research on Matter).

References

[1] Morosin B and Lingafelter E C 1961 *J. Phys. Chem.* **65** 50
[2] Clay R, Murray-Rust J and Murray-Rust P 1975 *Acta Crystallogr.* B **31** 289
[3] Gesi K and Iizumi M 1980 *J. Phys. Soc. Japan* **48** 1775
[4] Sawada A, Sugiyama J, Wada M and Ishibashi Y 1980 *J. Phys. Soc. Japan* **48** 1773
[5] Sugiyama J, Wada M, Sawada A and Ishibashi Y 1980 *J. Phys. Soc. Japan* **49** 1405
[6] de Wolff P M 1974 *Acta Crystallogr.* A **30** 777
[7] Janner A and Janssen T 1977 *Phys. Rev.* B **15** 643
[8] de Wolff P M, Janssen T and Janner A 1981 *Acta Crystallogr.* A **37** 625
[9] Janner A, Janssen T and de Wolff P M 1983 *Acta Crystallogr.* A **39** 671
[10] Janssen T 1986 *Ferroelectrics* **66** 203
[11] Hogervorst A C R 1986 Comparative study of the modulated structures in Rb_2ZnCl_4 and in related compounds *PhD Thesis* Delft
[12] Ortega J, Etxebarria J, Zubillaga J, Breczewski T and Tello M J 1992 *Phys. Rev.* B **45** 5155
[13] Madariaga G, Zúñiga F J, Paciorek W A and Bocanegra E H 1990 *Acta Crystallogr.* B **46** 620

[14] Kremers M, Dijkstra E and Meekes H 1994 *Phys. Rev.* submitted
[15] Meekes H and Janner A 1988 *Phys. Rev.* B **38** 8075
[16] Nye J F 1985 *Physical Properties of Crystals* (Oxford: Oxford University Press)
[17] Vlokh O G, Polovinko I I and Sveleba S A 1988 *Opt. Spektrosk.* **65** 751
[18] Vlokh O G, Dutsyak G Z, Kityk A V and Kityk I V 1990 *J. Appl. Spectrosc.* **53** 746
[19] Agranovich V M and Ginzburg V L 1974 *Crystal Optics with Spatial Dispersion and Excitons* (Berlin: Springer)
[20] Kobayashi J and Uesu Y 1983 *J. Appl. Crystallogr.* **16** 204
[21] Kremers M and Meekes H 1995 *J. Phys. D: Appl. Phys* **28** 1212
[22] Uesu Y and Kobayashi J 1985 *Ferroelectrics* **64** 115
[23] Hamano K, Ikeda Y, Fujimoto T, Ema K and Hirotsu S 1980 *J. Phys. Soc. Japan* **49** 2278
[24] Saito K, Sugiya H and Kobayashi J 1990 *J. Appl. Phys.* **68** 732
[25] Dijkstra E, Janner A and Meekes H 1992 *J. Phys.: Condens. Matter* **4** 693
[26] Kushnir O S and Vlokh O G 1993 *J. Phys.: Condens. Matter* **5** 7017
[27] Arend H, Perret F, Wüest H and Kerkoc P 1986 *J. Cryst. Growth* **74** 321
[28] Dijkstra E, Meekes H and Kremers M 1991 *J. Phys. D: Appl. Phys* **24** 1861
[29] Kremers M and Meekes H 1995 *J. Phys. D: Appl. Phys* **28** 1195
[30] Hedoux A, Grebille D, Lefebvre J and Perret R 1989 *Phase Transitions* **14** 177
[31] Vlokh O G, Zhmurko V S, Polovinko I I and Sveleba S A 1990 *Sov. Phys.-Tech. Lett.* **16** 900